Structure-Based Discovery of Triphenylmethane Derivatives as Inhibitors of Hepatitis C Virus Helicase[∞]

Chien-Shu Chen,[†,#] Chun-Tang Chiou,[†,●] Grace Shiahuy Chen,[‡] Sheng-Chia Chen,[§] Chih-Yung Hu,[§] Wei-Kuang Chi,[¶] Yi-Ding Chu,[¶] Lih-Hwa Hwang,[||] Pei-Jer Chen,[||] Ding-Shinn Chen,*[,||] Shwu-Huey Liaw,*[,§] and Ji-Wang Chern*[,†,⊥]

School of Pharmacy, College of Medicine, National Taiwan University, Taipei, Taiwan, Department of Applied Chemistry, Providence University, Shalu, Taiwan, Structural Biology Program, Faculty of Life Science, National Yang-Ming University, Taipei, Taiwan, Process Development Division, Development Center for Biotechnology, Taipei, Taiwan, Department of Internal Medicine, College of Medicine, Hepatitis Research Center, National Taiwan University Hospital, National Taiwan University, Taipei, Taiwan, and Department of Life Science, College of Life Science, National Taiwan University, Taipei, Taiwan

Received September 20, 2008

Hepatitis C virus nonstructural protein 3 (HCV NS3) helicase is believed to be essential for viral replication and has become an attractive target for the development of antiviral drugs. A fluorescence resonant energy transfer helicase assay was established for fast screening of putative inhibitors selected from virtual screening using the program DOCK. Soluble blue HT (**1**) was first identified as a novel HCV helicase inhibitor. Crystal structure of the NS3 helicase in complex with soluble blue HT shows that the inhibitor bears a significantly higher binding affinity mainly through a 4-sulfonatophenylaminophenyl group, and this is consistent with the activity assay. Subsequently, fragment-based searches were utilized to identify triphenylmethane derivatives for more potent inhibitors. Lead optimization resulted in a 3-bromo-4-hydroxyl substituted derivative **12** with an EC_{50} value of 2.72 μM to Ava.5/Huh-7 cells and a lower cytotoxicity to parental Huh-7 cells (CC_{50} = 10.5 μM), and it indeed suppressed HCV replication in the HCV replicon cells. Therefore, these inhibitors with structural novelty may serve as a useful scaffold for the discovery of new HCV NS3 helicase inhibitors.

Introduction

Hepatitis C virus (HCV[a]) is the major causative agent of chronic non-A and non-B hepatitis.[1] Patients with persistent HCV infection are at risk of developing liver cirrhosis and hepatocellular carcinoma.[2] The current recommended HCV treatment is a combination of interferon and ribavirin,[3] which, although effective, still has limitations of unsatisfactory response rates and significant adverse reactions.[4] Although pegylated interferon further improved the effectiveness, adverse reactions still exist and the cost is high.[5] In fact, around 50% of HCV genotype 1-infected patients fail to achieve a sustained virological response. Clearly, there is still a great need to develop more effective agents for the treatment of HCV infection.

The development of HCV antiviral agents has focused mainly on NS3/4A serine protease and NS5B RNA polymerase.[6−9] Although rapid and potent in inhibition of HCV replication, the development of resistance becomes the main issue just like with most antiviral drugs. Some of the potent HCV protease inhibitors[10] or NS5B polymerase inhibitors[11] have encountered drug resistance. Targeting a viral helicase required for viral replication might overcome the resistance problem.[12] HCV nonstructural protein 3 (HCV NS3) helicase plays an essential role in viral replication and, therefore, represents a potential antiviral drug target. Bisbenzimidazole derivatives were the first HCV helicase inhibitors reported with IC_{50} values ranging from 0.7 to 10 μM,[13] while their interactive mode is still uncertain.[14] Several 5-amino-1,2,4-thiadiazoliums were also reported as HCV helicase inhibitors with modest potency (IC_{50} = 25−75 μM).[15] By random sampling, halogenated benzotriazole[16] and benzotriazole nucleoside analogues[17] have been identified as HCV helicase inhibitors with IC_{50} values of 20 and 1.5 μM, respectively. Recently, a nucleotide-mimicking inhibitor QU663 was found as a potent selective HCV helicase inhibitor (K_i = 0.75 μM) by competing with the substrate.[18] In addition, intercalating agents epirubicin and nogalamycin are effective helicase inhibitors through the inhibition of RNA unwinding.[19] However, the high cytotoxicity excludes their application in HCV therapy.

Even though high-throughput screening has been used successfully toward the identification of new leads in drug discovery, it remains a costly and time-consuming process. Alternatively, virtual screening has emerged as a complementary approach.[20] The program DOCK[21] has been successfully applied in diverse protein systems for virtual screening. In the present study, we attempted to identify novel HCV NS3 helicase inhibitors by virtual screening of compound libraries using the

[∞] The coordinates and structure factors of HCV NS3 helicase in complex with compound **1** have been deposited in the RCSB Protein Data Bank, www.pdb.org (PDB code 2ZJO).

* To whom correspondence should be addressed. For S.-H.L.: phone, +886-2-28267278; fax, +886-2-28202449; e-mail, shliaw@ym.edu.tw. For D.-S.C.: phone, +886-2-23562176; fax, +886-23317624; e-mail, chends@ntu.edu.tw. For J.-W.C.: phone, +886-2-23939462; fax, +886-2-23934221; e-mail, jwchern@ntu.edu.tw.

† School of Pharmacy, College of Medicine, National Taiwan University.

Current address: School of Pharmacy, College of Pharmacy, China Medical University, Taichung, Taiwan.

● Current address: Division of Herbal Drugs and Natural Products, National Research Institute of Chinese Medicine, Taipei, Taiwan.

‡ Providence University.

§ National Yang-Ming University.

¶ Development Center for Biotechnology.

|| National Taiwan University Hospital, National Taiwan University.

⊥ College of Life Science, National Taiwan University.

[a] Abbreviations: HCV, hepatitis C virus; NS3, nonstructural protein 3; NS5B, nonstructural protein 5B; NTP, nucleoside triphosphate; FRET, fluorescence resonant energy transfer; ATP, adenosine triphosphate; ss RNA, single-stranded RNA; RT-PCR, reverse transcription-PCR.

10.1021/jm8011905 CCC: $40.75
Published on Web 04/14/2009

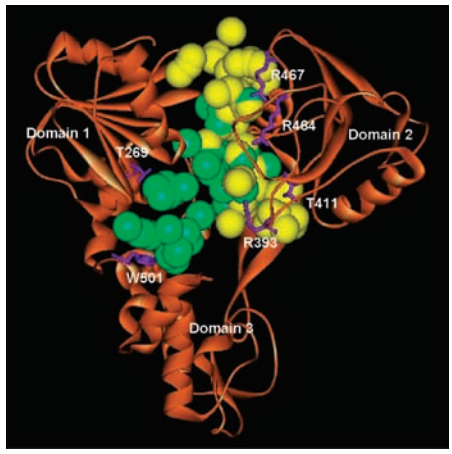

Figure 1. DOCK screens were carried out in docking sites I and II. The docking site was defined with a set of spheres (green and yellow for sites I and II, respectively) that were used to orient a putative ligand molecule.

program DOCK, followed by activity assay and structural characterization.

Results and Discussion

Virtual Screening. The crystal structures of HCV NS3 show a Y-shaped configuration consisting of three structural domains.[22,23] Domains 1 and 3 share an extensive interface mainly through packing of the three helices, and they form a hollow interface. On the other hand, domain 2 is distinctly separated from the other two domains and gives rise to a series of clefts. All the conserved motifs are clustered around the interdomain interfaces. Two conserved residues, Arg464 and Arg467, in domain 2 are expected to move toward the conserved NTP-binding loops in domain 1, leading to closure of the interdomain cleft upon nucleoside triphosphate (NTP) binding.[24] Crystal structure[23] and mutagenesis[25] studies revealed that some critical amino acid residues, such as Thr269, Trp501, Arg393, and Thr411, are important for nucleic acid binding. It was our intention to find potential inhibitors by blocking the closing of the interface between domains 1 and 2. Therefore, two docking sites I and II close to the conserved motifs and the putative substrate-binding residues were defined (Figure 1).

Fourteen compounds were chosen and subjected to HCV helicase inhibition assays. Among them, soluble blue HT (**1**, Chart 1), screened from site II, inhibited the HCV NS3 helicase activity with an IC_{50} value of 40 μM, and *N*-(2-pyrimidinyl)-benzenesulfonamide derivative **2**, screened from site I, possessed a 46% inhibition at 100 μM against HCV NS3 helicase (Table 1). The other 12 compounds had no inhibitory effects. To identify the attenuation mechanism of soluble blue HT, the complex structure with a HCV NS3H helicase domain was determined.

Establishment of Helicase Assay System. A fluorescence resonant energy transfer (FRET) helicase assay system was established for fast screening of the HCV NS3/4A helicase inhibitors selected from virtual screening. The fluorescence intensity increased in a time-dependent manner in the reaction with NS3/4A, while it remained at the basal level in the reaction without NS3/4A. The solvent dimethyl sulfoxide had no effect on the helicase activity.

Soluble Blue HT-Binding Site. The present inhibitor complex possesses a wider cleft between domains 1 and 2 and hence can be described as an "open" conformation (Figure 2A), whereas there is a narrower cleft in the NS3 and a single-stranded deoxyoligonucleotide dU_8 complex that can be described as a "closed" conformation. Superimposition of the available HCV NS3 helicase structures revealed two conformations with a rigid-body rotation of domain 2 (20−25°) relative to domains 1 and 3 (Figure 2B).

In the initial $F_o - F_c$ omit map contoured at the 5σ level, only one strong electron density was observed and assigned as the 4-sulfonatophenylaminophenyl group and an adjacent phenyl ring. Significant density maps for the two adjacent 3-sulfonatophenylamino moieties were observed at 4σ and 3σ levels, respectively (Figure 3A). The 4-sulfonatophenylaminophenyl group is the key component for the inhibitor binding through its interaction with the conserved motif I (residues 207−212) and the second helix (residues 233−241) (Figure 3B). The most significant interactions are hydrogen bonds formed between the sulfonate group and the backbone NH groups of Gly207, Gly209, Lys210, Ser211, and Thr212 and Thr212 $O^{\gamma 1}$. The phenyl ring between the sulfonate and amino groups makes close contacts with Thr206 $C^{\gamma 2}$, Phe238 $C^{\varepsilon 1}$ and Tyr241 C^{γ}. The amino group interacts with Gly237 O, and the second phenyl group has close interactions with Ala234 C^{β} and Gly237 C^{α}. A phenyl ring in one adjacent 3-sulfonatophenylamino group makes contact with Ala233 C^{β} and Ala234 C^{α}. The remaining parts of blue HT have no significant interactions with this "open" conformation. However, in the "closed" conformation, the other 3-sulfonatophenylamino group might interact with the conserved motif V such as Met415 and Thr416 in domain 2. The enzyme undergoes only minor conformational changes upon inhibitor binding. In addition to the physical interactions mentioned above, shape complementarity also plays an important role in facilitating the specific binding between protein and inhibitor (Figure 3C). The inhibitor was bound in a shallow binding groove made up of the conserved motif I and the first two helices. One of the main topological features is that the sulfonate group is situated at the 4-position of the phenylamino group.

Triphenylmethane Derivatives as Novel Inhibitors of HCV NS3 Helicase. Soluble blue HT (**1**) represents a novel lead compound for HCV NS3 helicase inhibitors. Therefore, a fragment-based search was commenced to find compounds related to the 4-sulfonatophenylaminophenyl group, the key character binding to the enzyme, as a query (fragment A in Chart 1). Among the hits, compound **3** was found to be more potent than compound **1** with an IC_{50} value of 12.6 μM against HCV NS3 helicase. The structures of compounds **1** and **3** suggest that the triphenylmethyl moiety may be essential for the inhibitory activity. Hence, another fragment-based search was carried out using fragment B (Chart 1), in which the triphenylmethyl moiety is linked to a phenyl ring through one atom. Compounds **4** and **6** showed moderate HCV helicase inhibition with IC_{50} values of 29.7 and 13.9 μM, respectively, while **5** was not active. The inactivity of the 4-nitrophenyloxytriphenyl derivative **5** reveals that a nitro group and a bridging oxygen are not appropriate at the positions.

Compounds **7**−**10** (Chart 2) were used to study the structural characteristics for the inhibitory activity of compound **6**. Compounds containing tri(4-hydroxylphenyl)methyl (**7**) and tri(4-aminophenyl)methyl skeleton (**8**) showed weak HCV helicase inhibition (39% and 30% inhibition at 100 μM, respectively, Table 1). These results indicate that the triphenylmethyl moiety alone could not achieve a high-affinity binding to the enzyme. An extended phenyl moiety, such as the 4-sulfonatophenylamino group in compounds **1** and **3**, would improve the binding affinity. As a result, the 2-(4-hydroxyphenyl)propane moiety of compound **6** might play an important

Chart 1. Compounds **1** and **2** Identified from the DOCK Screening and Fragments A and B Used for the Fragment Search

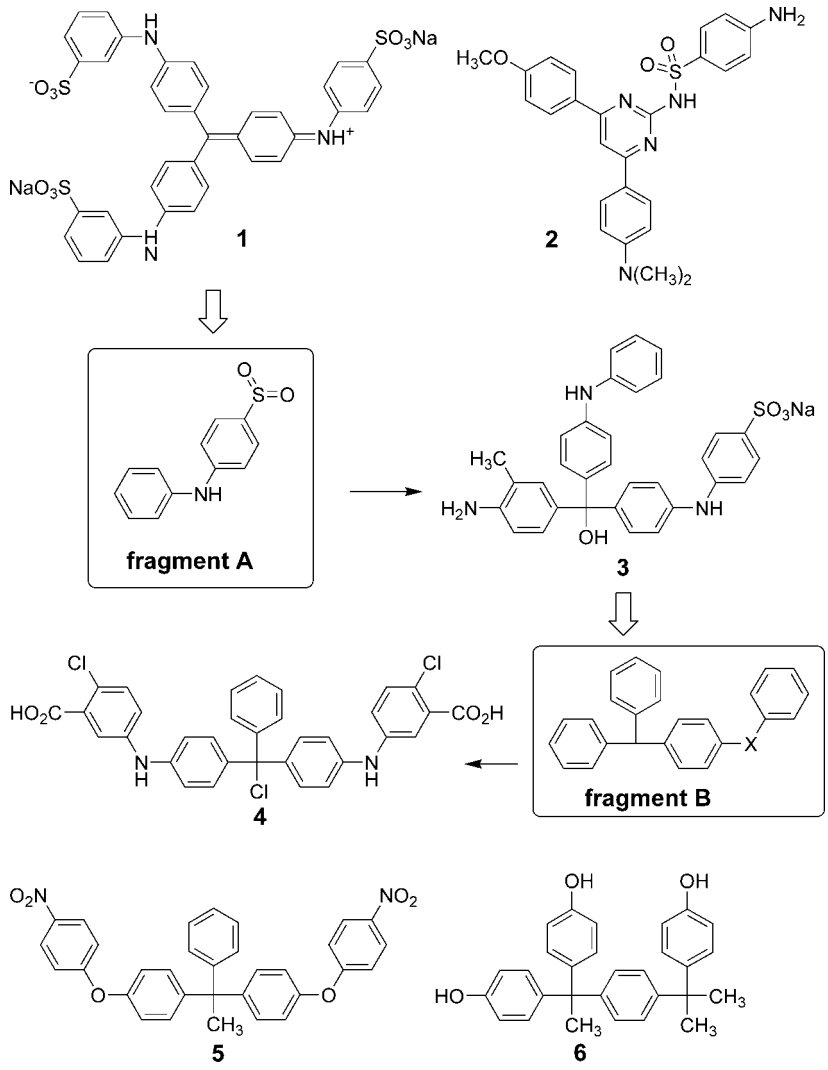

role responsible for the potency. Further evidence was attained by compound **10** in which a hydroxyphenyl group was replaced by a methyl group. Compound **10** exhibited less potency (IC_{50} = 60.7 μM), but it was more potent than compounds **7**−**9**. Therefore, the triphenylmethane moiety can serve as a basic scaffold for the inhibitory potency against HCV helicase. Together with extended moieties, compound **6** may represent a novel lead structure for the HCV helicase inhibitors.

Attenuation Mechanism. The unwinding ability of HCV helicase is dependent on adenosine triphosphate (ATP) binding, ATP hydrolysis, and RNA binding. To examine the inhibition mechanism of compounds **1**, **3**, **4**, and **6**, their inhibitory effects on ATPase activity and RNA substrate binding were examined. Compounds **1**, **4**, and **6** inhibited the ATP activity with IC_{50} values of about 25 μM in a mixed type mode, while compound **3** had little effect (Figure 4A and Table 1). Compound **1**, **3**, **4**, and **6** all inhibited the RNA substrate binding to the HCV NS3/4A helicase in a dose dependent manner (Figure 4B). Compound **1** showed high interference on the RNA substrate binding. Compounds **4** and **6** exhibited a similar effect, while compound **3** had the weakest interfering effect.

Table 1. Inhibition of the Unwinding Activity of HCV Helicase and ATPase Activity

	IC_{50} (μM)			
compd	helicase	ATPase	compound	IC_{50} (μM), helicase
1	40.0	23.8	**7**	39%[a]
2	46%[a]	nd[b]	**8**	30%[a]
3	12.6	>100	**9**	43%[a]
4	29.7	25.1	**10**	60.7
5	0%[a]	nd[b]	**11**	15%[a]
6	13.9	25.9	**12**	10.1

[a] Percent inhibition at 100 μM. [b] Not determined.

Unexpectedly, compound **3**, the most potent compound in the FRET helicase activity assay, showed little inhibition in ATP hydrolysis or RNA substrate binding. It was known that DNA substrate was easier unwound than RNA substrate in the helicase activity assay. Thus, the inhibitory activity of these compounds was further investigated by the helicase assay with isotope-labeled RNA substrates. At a concentration of 100 μM, compounds **1**, **4**, and **6** totally blocked the formation of single-stranded (ss) RNA (Figure 4C). On the other hand, compound **3** showed little effects on the formation of ss RNA, suggesting that compound **3** could not inhibit RNA unwinding.

Antiviral Activity in HCV Replicon Cells. Antihepatitis C virus activities of compounds **1**, **3**, **4**, and **6** were further analyzed in HCV replicon Ava.5/Huh-7 and its parental Huh-7 cells (Table 2). Compounds **1** and **4** were not toxic to either cells. Compound **3** exhibited high cytotoxicity to HCV replicon with an EC_{50} value of 0.69 μM and to parental Huh-7 cells with a CC_{50} value of 0.96 μM. Compound **6** showed moderate

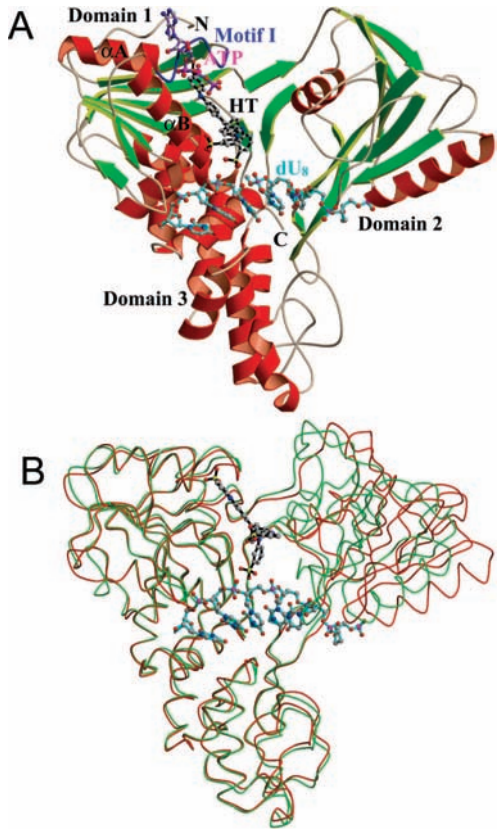

Figure 2. (A) Present HCV NS3 helicase structure in complex with blue HT (**1**) and models of the cofactor ATP and a single-stranded deoxyoligonucleotide dU_8 (cyan). The dU_8 and ATP models were generated through superposition with the NS3-dU_8 complex (PDB 1A1V) and the helicase RecQ (PDB 1OYY), respectively. The 4-sulfonatophenylaminophenyl group contributes most to the binding, and it is bound in a shallow groove constituted by the conserved motif I, the first two helices (αA and βB), and the β-sheet in domain 1. Helices in the NS3 structure are in red and strands in green, and the motif I is highlighted in blue. The blue HT, ATP, and dU_8 are shown as ball-and-stick representation with black, purple, and cyan carbons, respectively. (B) Two conformations of NS3H structures. The present structure is in red and described as an "open" conformation, whereas the NS3H-dU_8 complex in green is described as a "closed" conformation. The structures are superimposed along domains 1 and 3 to demonstrate the relative orientation of domain 2.

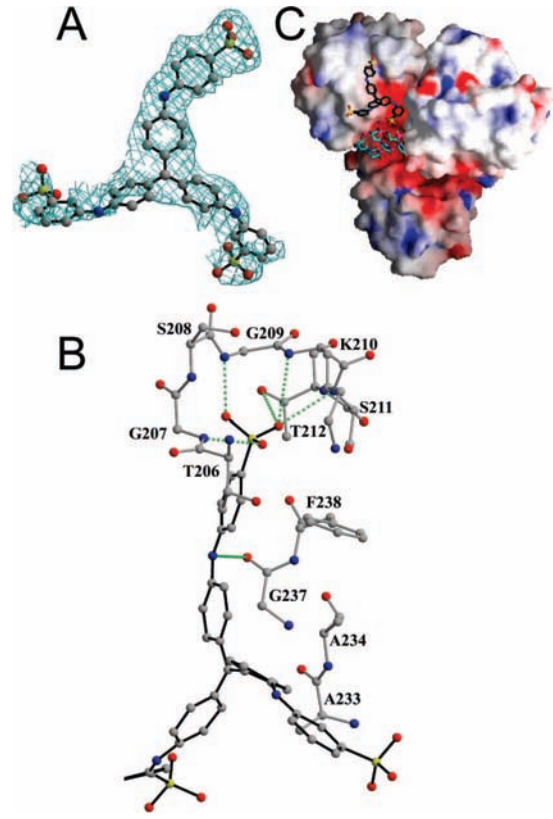

Figure 3. Blue HT-binding site. (A) The initial simulated annealing omitting $F_o - F_c$ map for the blue HT (**1**) bound to NS3H contoured at the 3σ level and shown in cyan. (B) The NS3 helicase-blue HT interactions. Hydrogen bonds are indicated by dashed lines. (C) Molecular surfaces of NS3H colored for electrostatic potential from -10 k_BT (red) to 10 k_BT (blue).

Chart 2. Compounds for the Identification of the Structural Characteristics of **6**

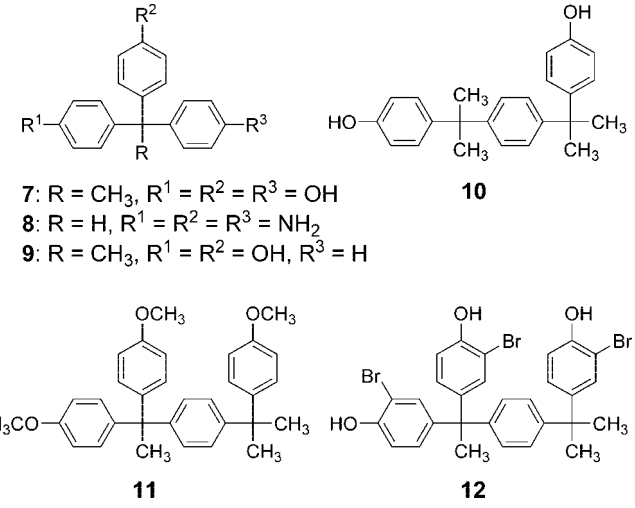

cytotoxicities to HCV replicon with an EC_{50} value of 8.37 μM and to Huh-7 cells with a CC_{50} value of 12.66 μM.

Lead Optimization. Compound **6** exhibited moderate inhibitory activity against HCV helicase with either DNA or RNA substrate. Therefore, lead optimization on the structure of compound **6** was performed. Methylation of the three hydroxyl groups leading to compound **11** (Chart 2) resulted in the loss of HCV helicase inhibitory activity (Table 1). This result reveals the importance of the 4-hydroxyl groups. Among various derivatives of compound **6**, the 3-bromo-4-hydroxyl substituted derivative **12** appeared to be the best candidate as a HCV helicase inhibitor. Compound **12** showed a good inhibitory activity against HCV NS3/4A helicase with an IC_{50} value of 10.05 μM and presented a better antiviral activity with an EC_{50} of 2.72 μM to Ava.5/Huh-7 cells and a lower cytotoxicity to parental Huh-7 cells (CC_{50} = 10.5 μM).

The antihepatitis C virus activity of compound **12** was further confirmed by real-time reverse transcription-PCR (RT-PCR). Compared to untreated Ava.5/Huh-7 cells, the HCV RNA decreased about 40−60% when cells were treated with 5 or 10 μM compound **12** for 2 days (Figure 5), indicating that compound **12** indeed suppressed HCV replication in the HCV replicon cells. In addition, a reduction of 20−25% of cell growth was found in the treatment of compound **12** at 5 μM with Ava.5/Huh-7 cells for 5 days without G418, an antibiotic blocking polypeptide synthesis through the inhibition of the elongation step in both prokaryotic and eukaryotic cells, while a reduction of 50−60% of cell growth was found in the same experiment with G418. These results illustrate that compound **12** has only minimal effects on the growth of proliferating cells but a major

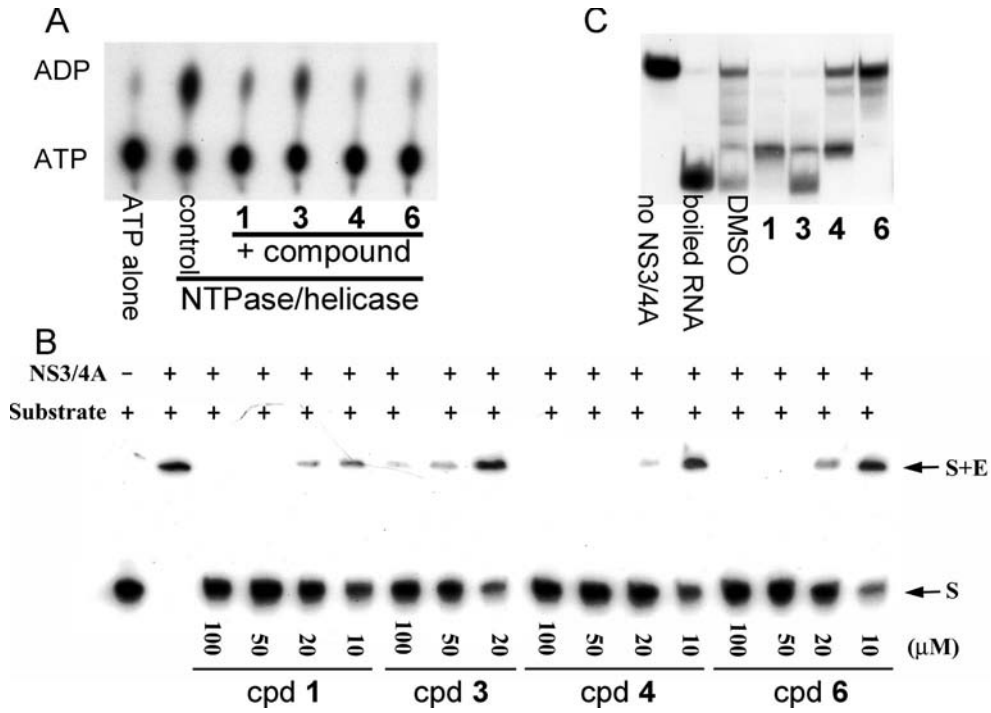

Figure 4. (A) Inhibition of the ATPase activity at a concentration of 100 μM, (B) inhibition of the RNA substrate (S) binding to the NS3/4A enzyme (E) at different concentrations, and (C) helicase activity with isotope labeled RNA substrate at a concentration of 100 μM by compounds **1**, **3**, **4**, and **6**. In the isotope-labeled helicase assay (C), some intermediate bands between the bands of double-stranded (ds) and single-stranded (ss) RNA were found.

Table 2. Antiproliferative Effects on Huh-7 and HCV Replicon Ava.5/Huh-7 Cells

compd	CC_{50} (μM), Huh7	EC_{50} (μM), Ava.5/Huh-7	specificity
1	>50.00	>50.00	
3	0.96	0.69	1.39
4	>50.00	>50.00	
6	12.66	8.37	1.51
12	10.50	2.72	3.86

influence on the replicon replication. The inhibition of Ava.5/Huh-7 cells was a consequence of inhibiting replicon replication.

Conclusion

Triphenylmethane derivatives were discovered as novel HCV NS3 helicase inhibitors through a consensus virtual screening of docking and fragment-based search. Compound **6**, a triphenylmethane derivative linked to a 2-(4-hydroxyphenyl)propane moiety, was identified as a HCV helicase inhibitor through the inhibition of ATPase hydrolysis and RNA substrate binding. Lead optimization advanced the discovery of compound **12**, 3-bromo substituted derivative of compound **6**, as a good anti-HCV agent with an IC_{50} value of 10.05 μM and EC_{50} value of 2.72 μM against HCV NS3 helicase and replicon Ava.5/Huh-7 cells, respectively. Results of real-time RT-PCR confirmed that compound **12** could suppress HCV RNA replication in the HCV replicon cells. Therefore, these inhibitors with structural novelty may serve as novel leads for the discovery of new HCV NS3 helicase inhibitors. Further lead optimization should be carried out for more potent HCV helicase inhibitors.

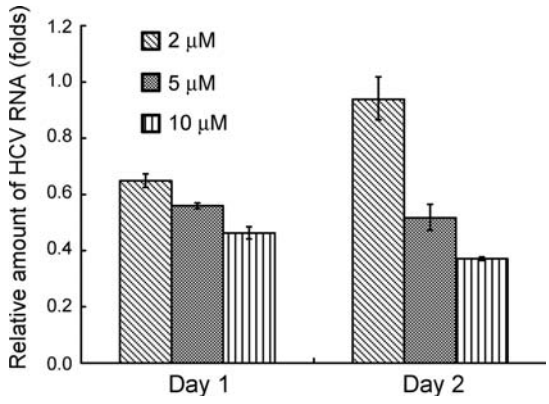

Figure 5. HCV RNA. HCV replicon cells were treated at various concentrations with compound **12** for 1 or 2 days. The amount of HCV RNA was analyzed by the real-time RT-PCR method. The RNA of untreated replicon cells was set as 1.0.

Experimental Section

Virtual Screening. Docking Screening. The X-ray crystal structure of HCV helicase (1HEI) was used for docking screening. The shape complementarity (contact) scoring function in the rigid-body docking (DOCK 3.5) was used to screen the database Available Chemicals Directory (ACD, version 99.1, Molecular Design Limited Information Systems, CA). The three-dimensional structures of the ACD compounds were generated using the CONCORD program (Tripos, Inc., MO). The top 1000 ranked molecules were redocked using the force field (energy) scoring function. All calculations were performed on a Silicon Graphics O2 workstation with a 180 MHz R5000 processor (SGI, CA). For compound selection, the docking models of the 1000 top-ranked compounds obtained by contact scoring were visually inspected using the software Insight II (Accelrys Inc., San Diego, CA). Together with consideration of chemical diversity, the selection of compounds was assisted by visual analysis of the docking models with respect to shape fitting and hydrogen-bonding and hydrophobic interactions. The compounds considered were also inspected for their favorable docking poses obtained by force field scoring. Finally, 14 compounds were selected for HCV helicase inhibition assay: 10 compounds from site I screening and 4 compounds from site II screening. The compounds for testing were purchased from chemical suppliers.

Fragment-Based 2D Database Searching. The fragment-based 2D search was carried out by the program ISIS/Base 2.2 (MDL Information Systems, Inc., CA). Two MDL databases, Screening Compounds Directory (SCD, version 2001.2) and ACD (version 2001.1), were searched with query structures. Compounds **3**−**5** were retrieved from SCD, and compounds **6**−**10** were found from ACD.

Synthesis and Characterization. Material and Methods. All solvents and reagents were used as obtained. Melting points were determined on a capillary melting point apparatus equipped with a digital thermometer and are uncorrected. NMR spectra were recorded at Bruker DPX 400 MHz with solvents as internal references. Mass spectra were determined using electron spray impact ionization at 70 eV on Finnigan Mat-TSQ 7000. Compounds **1**−**10** were used as purchased, and their purity was >90%. Purity of compounds **11** and **12** was determined using a Hitachi D-7000 HPLC instrument, and these compounds were >95% pure.

1-[1,1-Bis(4-methoxyphenyl)ethyl]-4-[2-(4-methoxyphenyl)-propan-2-yl]benzene (11). To a solution of compound **6** (0.5 g, 1.18 mmol) in acetone (15 mL) were added K_2CO_3 (0.55 g, 3.98 mmol) and CH_3I (0.25 mL, 4.02 mmol). The mixture was stirred at room temperature for 24 h. The mixture was filtered, and the filtrate was evaporated under reduced pressure. The resulting residue was subjected to column chromatography on silica gel (70−230 mesh), eluting with hexanes/EtOAc (95:5) to give **11** (75 mg, 14%) as a white solid: mp 98−99 °C; ^{1}H NMR (400 MHz, $CDCl_3$) δ 1.76 (s, 6H, CH_3), 2.22 (s, 3H, CH_3), 3.90 (s, 9H, OCH_3), 6.90 (d, J = 8.6 Hz, 4H, ArH), 6.92 (d, J = 8.5 Hz, 2H, ArH), 7.07 (d, J = 8.4 Hz, 2H, ArH), 7.11 (d, J = 8.7 Hz, 4H, ArH), 7.21 (d, J = 8.4 Hz, 2H, ArH), 7.28 (d, J = 8.6 Hz, 2H, ArH); MS (ESI^+) m/z 489 $[M + Na]^+$.

4-[1-(3-Bromo-4-hydroxyphenyl)-1-[4-[2-(3-bromo-4-hydroxyphenyl)propan-2-yl]phenyl]ethyl]-2-bromophenol (12). According to the method by Oberhauser,[26] compound **6** (0.8 g, 1.88 mmol) was dissolved in a mixture of CH_3CN (15 mL), CH_2Cl_2 (5 mL), and acetone (1 mL). To the stirred solution under ice bath were added CF_3SO_3H (0.55 mL, 6.26 mmol) and NBS (0.55 g, 3.09 mmol). Additional NBS (0.55 g, 3.09 mmol) was added to the mixture after 10 min, and stirring was continued for 10 min under ice bath and then at room temperature for 3 h. A solution of $NaHSO_3$ (4 g) in H_2O (15 mL) was added, and the mixture was extracted with CH_2Cl_2 (20 mL in total). The extract was washed with H_2O (15 mL) twice and brine (15 mL). After evaporation, the residue was dissolved in 3 N NaOH (10 mL), and the solution was added dropwise with stirring to 3 N HCl (20 mL). The resulting precipitate was collected by filtration and washed with H_2O to give **12** (1.09 g, 88%). An analytical sample was prepared by flash chromatography on silica gel (230−400 mesh), eluting with hexanes/EtOAc (70:30): mp 81−84 °C; ^{1}H NMR (400 MHz, DMSO-d_6) δ 1.56 (s, 6H, CH_3), 1.98 (s, 3H, CH_3), 6.80−6.87 (m, 5H, ArH), 6.91 (d, J = 8.4 Hz, 2H, ArH), 6.99−7.01 (m, 3H, ArH), 7.13 (d, J = 8.5 Hz, 2H, ArH), 7.22 (d, J = 2.2 Hz, 1H, ArH), 10.00 (brs, 1H, OH), 10.14 (brs, 2H, OH). HRMS (ESI^-) calcd for $C_{29}H_{24}Br_3O_3$ $[M - H]^-$: 656.9276 ($^{79}Br_3$), 658.9255 ($^{79}Br_2{}^{81}Br$); found 656.9304 ($^{79}Br_3$), 658.9296 ($^{79}Br_2{}^{81}Br$).

Fluorescence Resonant Energy Transfer (FRET) Helicase Assay. The high throughput assay system was modified from a previous report.[27] The histidine-tag HCV NS3/4A protein was expressed and purified as previously described.[28] As purified NS3 helicase presents DNA helicase activity,[29,30] a double-stranded oligomeric DNA with a 3′ flanking sequence was used as the substrate.[31] The template strand (5′-CATCATGCAGGACAGTCG-GATCGCAGTCAG-3′), the release strand (5′-CTGTCCTGCAT-GATG-3′), and the trapping strand (5′-CATCATGCAGGACAG-3′) were synthesized by Sigma-Proligo (Singapore). A quencher BHQ1 was labeled at the 3′ end of the release strand, and a fluoresceinisothiocyanate (FITC) was labeled at the 5′ end of the template strand. The release and template strands were mixed in a molar ratio of 1:1. The mixture (30 μM) was boiled for 10 min and cooled to room temperature overnight for annealing. The annealing of BHQ1-labeled release strand and FITC-labeled template strand was monitored by the fluorescence quenching of FITC.

NS3/4A (0.9 μg) was incubated with compounds on ice for 15 min and then mixed with 1 μM DNA substrate and 10 μM trapping strand in reaction buffer (20 mM HEPES−KOH (pH 7.0), 2 mM DTT, 0.1 mg/mL BSA, 2.5 mM ATP, and 1.5 mM $MgCl_2$). The mixture with a final compound concentration of 100 μM was added to a 384-well microplate and monitored continuously at an excitation of 485 nm and an emission of 518 nm using a Fluoroskan Ascent microplate fluorescence reader (LabSystems, VA). The original data were normalized by the formula "relative helicase activity (%) = $(F_{de} - F_{d0})/(F_{De} - F_{D0})$" where F_{de} and F_{d0} are the fluorescence intensity of reaction with compounds at the end point and at the beginning, respectively, F_{De} and F_{D0} are the fluorescence intensity with dimethyl sulfoxide (DMSO) at the end point and at the beginning, respectively. When the inhibition of helicase activity was more than 50% at a concentration of 100 μM, the IC_{50} values were determined with the compound concentrations of 100, 50, 20, and 10 μM by fitting SigmaPlot2000 of logistic with three parameters.

Helicase Activity Assay with Isotope-Labeled RNA Substrate. The isotope-labeled partial double-stranded RNA (dsRNA) substrates were prepared, and RNA helicase assays were conducted following the reported procedures.[29,30] NS3/4A (0.45 μg) was incubated with a compound on ice for 15 min. The reaction mixture (20 μL) contained 20 mM HEPES−KOH (pH 7.0), 2 mM DTT, 1.5 mM $MnCl_2$, 2.5 mM ATP, 0.1 mg/mL BSA, 20 U of RNasin, and 30 nM dsRNA substrate. The reaction was carried out at 37 °C for 1 h and then terminated by adding 5 μL of RNA loading dye (0.1 M Tris-HCl (pH 7.4), 20 mM EDTA, 1% SDS, 0.1% bromophenol blue, 0.1% xylene cyanol, and 50% glycerol). The reaction products were analyzed on an 8% native polyacrylamide gel.

ATP Activity Assay. Following our previous report,[28] compounds were added into the reaction buffer (20 mM HEPES−KOH (pH 7.0), 1.5 mM $MgCl_2$, 2 mM DTT, 0.1 μg/mL poly-U, and 5 μCi [α-^{32}P]ATP containing 0.067−20 μM ATP). The reaction was initiated by addition of NS3/4A (0.45 μg) and was terminated after 5 min by addition of 0.5 μL of 0.4 M EDTA (pH 8.0). A sample of 0.5 μL of reaction mixture was spotted on a PEI-cellulose-F TLC plate (Merck, Darmstade, Germany) and developed by ascending chromatography in 0.375 M K_2PO_4 (pH 3.5) for 20 min. The TLC plate was then air-dried and applied to autoradiography measured by the AutoChemi Imaging System (UVP, Inc., CA).

RNA Binding Assay. Partial dsRNA binding to HCV helicase was analyzed by gel mobility shift assay.[30] NS3/4A (0.45 μg) was incubated with 100 μM tested compounds in 10 μL of helicase reaction buffer in the absence of ATP for 5 min at 37 °C and then incubated with 0.66 pmol of isotope-labeled partial dsRNA substrate for further 15 min. Reaction products were analyzed on a 4% polyacrylamide gel containing 5% glycerol. The bound complexes were visualized by autoradiography.

Real-Time RT-PCR. HCV replicon cells Ava.5/Huh-7 carrying a genotype 1b[32] were seeded on culture dishes and cultured with G-418-free DMEM medium for 24 h. Cells were then treated with 5, 10, or 20 μM compound **12** and cultured for further 24 or 48 h. Cells were lysed with RNA-Bee (Tel-Test Inc.) to obtain cellular total RNA. Purified RNA was quantified and frozen at −80 °C.

The synthesis of the first strand cDNA was accomplished by 1 μg of RNA applied to Reverse-iT first strand synthesis kit (ABgene). A mixture (12 μL) containing RNA and random decamers (400 ng) was heated at 70 °C for 5 min and then placed on ice to remove secondary structures. Then the mixture was combined with another mixture (8 μL) containing buffer, dNTP, enzyme, and DTT, followed by incubation at 47 °C for 50 min. When the reaction was completed, the mixture was heated at 75 °C for 10 min to inactivate the enzyme and then stored at −20 °C.

The first strand cDNA was applied to ABsolute QPCR SYBR Green Mixes (ABgene) for real-time PCR reaction, and the primer set was generated by the software of PrismExpress (Applied

Table 3. Statistics for Data Collection and Structural Refinement

parameter	
space group	$P3_121$
unit cell (Å)	92.06, 104.71
resolution range (Å)	50−2.5
total observations	199 340
unique reflections	17 989
completeness (%)	99.8
$I/\sigma\langle I\rangle$	36.3
R_{merge} (%)	6.5
R_{cryst} for 90% data (%)	23.4
R_{free} for 10% data (%)	28.3
rms deviations of bond lengths and bond angles	0.08 Å, 1.5°

Biosystems, CA). The sequences of the HCV primer set were 5′-^{233}gtgcccccgcgagact^{248}-3′ (forward) and 5′-^{305}agcaccctatcaggcagtacca^{284}-3′ (reverse). The primer set consisting of 5′-^{943}acccactcctccacctttga^{962}-3′ (forward) and 5′-^{1018}cataccaggaaatgagcttgacaa^{995}-3′ (reverse) is used for internal control gene GAPDH. A mixture (12.0 μL) containing 1 μL of the first strand cDNA was mixed with 12.5 μL of master mix and 0.5 μL of primer set and applied to ABI Prism 7900 for the real-time PCR reaction. The enzyme of real-time PCR was activated at 95 °C for 15 min, and then PCR reaction was performed with 40 cycles of denature at 95 °C for 15 s and annealing/extension at 60 °C for 1 min, followed by a dissociation stage to verify the specificity of the reaction. The values for HCV primer set were normalized to those of GAPDH (Applied Biosystems). Each test was done in triplicate, and averages were obtained.

Structure Determination. The NS3 helicase domain from a Taiwanese HCV strain (genotype 1b) was expressed using the pET21a vector in *E. coli* BL21 (DE3).[29,30] The recombinant enzyme was crystallized by the hanging-drop vapor diffusion method at 22 °C. The hanging drops were mixtures of 2 μL of reservoir solution and 2 μL of protein solution (15 mg/mL). Protein crystals were grown in 0.2 M KCl, 0.1 M $Mg(OAc)_2$, 10% PEG 8000, and 0.05 M sodium cacodylate (pH 6.5). Compound derivatives were prepared by soaking crystals in reservoir solution containing compound at various concentrations (1−100 mM) for various lengths of time ranging from 1 h to a couple of days.

X-ray diffraction data were collected at 100 K with addition of 30% glycerol as a cryoprotectant, using synchrotron radiation at beamline 13B1, National Synchrotron Radiation Research Center, Taiwan. The data were processed using the HKL2000 program.[33] The crystals belong to the space group $P3_121$, with one helicase domain per asymmetric unit. The complex structure was determined by a combination of molecular replacement and single isomorphous replacement methods. Initial attempts to solve the structure using the available NS3H structures as starting models failed. Structural comparison revealed two conformations, which differed primarily with regard to the relative orientations of domains 1 and 3 and domain 2. Thus, the NS3H model was split into the three structural domains (residues 190−330 for domain 1; residues 327−435 and residues 450−485 for domain 2; residues 430−450 and residues 485−625 for domain 3). Rotation and translation function searches were performed with the program AMORE. Clear solutions for domains 1 and 3 but not for domain 2 were observed. The phase for the domain 2 was solved together with a thimerosal derivative, in which a mercury ion was bound at Cys 420. The complex structures were solved by molecular replacement and underwent straightforward refinement against the data to 2.5 Å resolution using the program CNS.[34] The N-terminal residues including a 12-residue vector linker and residues 167−186 as well as the C-terminal hexahistidine tag exhibited no electron density and were omitted in the final model. Only faint electron densities were observed for residues 393−400 and 416−420. Data collection and refinement statistics are depicted in Table 3. Figure 2 and Figure 3B were generated by MolScript.[35] Figure 3A was made by BobScript,[35] and Figure 3C was obtained by Grasp.[36]

Acknowledgment. We thank Dr. Bhalchandra V. Bhagwat and Chao-Wu Yu for their technical assistance and Apath LLC (St. Louis, MO) for the agreement to use HCV replicon Ava.5 cells. This study was supported by National Science Council of the Republic of China (Grants NSC91-2321-B-002-002, NSC93-2323-B-002-015, and NSC95-2323-B-002-009).

Supporting Information Available: Purity data from HPLC analysis and ^{1}H NMR spectrum of compound **12**. This material is available free of charge via the Internet at http://pubs.acs.org.

References

(1) Choo, Q. L.; Kuo, G.; Weiner, A. J.; Overby, L. R.; Bradley, D. W.; Houghton, M. Isolation of a CDNA clone derived from a blood-borne non-A, non-B viral-hepatitis genome. *Science* **1989**, *88*, 359–362.
(2) Jenny-Avital, E. R. Hepatitis C. *Curr. Opin. Infect. Dis.* **1998**, *11*, 293–299.
(3) Chander, G.; Sulkowski, M. S.; Jenckes, M. W.; Torbenson, M. S.; Herlong, H. F.; Bass, E. B.; Gebo, K. A. Treatment of chronic hepatitis C: a systematic review. *Hepatology* **2002**, *36*, S135–S144.
(4) Lai, M. Y.; Kao, J. H.; Yang, P. M.; Wang, J. T.; Chen, P. J.; Chan, K. W.; Chu, J. S.; Chen, D. S. Long-term efficacy of ribavirin plus interferon alfa in the treatment of chronic hepatitic C. *Gastroenterology* **1996**, *111*, 1307–1312.
(5) Hadziyannis, S. J.; Sette, H.; Morgan, T. R.; Balan, V.; Diago, M.; Marcellin, P.; Ramadori, G.; Bodenbeimer, H.; Bemstein, D.; Rizzetto, M.; Zeuzem, S.; Pockros, P. J.; Lin, A.; Ackrill, A. M. Peginterferon-alpha 2a and ribavirin combination therapy in chronic hepatitis C. A randomized study of treatment duration and ribavirin dose. *Ann. Intern. Med.* **2004**, *140*, 346–355.
(6) Steinkuehler, C.; Koch, U.; Narjes, F.; Matassa, V. G. Hepatitis C virus serine protease inhibitors: current progress and future challenges. *Curr. Med. Chem.* **2001**, *8*, 919–932.
(7) Gordon, C. P.; Keller, P. A. Control of hepatitis C: a medicinal chemistry perspective. *J. Med. Chem.* **2005**, *48*, 1–20.
(8) Neyts, J. Selective inhibitors of hepatitis C virus replication. *Antiviral Res.* **2006**, *71*, 363–371.
(9) Qureshi, S. A. Hepatitis C virus. Biology, host evasion strategies, and promising new therapies on the horizon. *Med. Res. Rev.* **2007**, *27*, 353–373.
(10) Lin, C.; Lin, K.; Luong, Y. P.; Rao, B. G.; Wei, Y. Y.; Brennan, D. L.; Fulghum, J. R.; Hsiao, H. M.; Ma, S.; Maxwell, J. P.; Cottrell, K. M.; Perni, R. B.; Gates, C. A.; Kwong, A. D. In vitro resistance studies of hepatitis C virus serine protease inhibitors. VX-950 and BILN 2061: structural analysis indicates different resistance mechanisms. *J. Biol. Chem.* **2004**, *279*, 17508–17514.
(11) Nguyen, T. T.; Gates, A. T.; Gutshall, L. L.; Johnston, V. K.; Gu, B.; Duffy, K. J.; Sarisky, R. T. Resistance profile of a hepatitis C virus RNA-dependent RNA polymerase benzothiadiazine inhibitor. *Antimicrob. Agents Chemother.* **2003**, *47*, 3525–3530.
(12) Kwong, A. D.; Rao, B. G.; Jeang, K. T. Viral and cellular RNA helicases as antiviral targets. *Nat. Rev. Drug Discovery* **2005**, *4*, 845–853.
(13) Diana, G. D.; Bailey, T. R. Compounds, Compositions and Methods for Treatment of Hepatitis C. U.S. Patent 5,633,388, 1997.
(14) Phoon, C. W.; Ng, P. Y.; Ting, A. E.; Yeo, S. L.; Sim, M. M. Biological evaluation of hepatitis C virus helicase inhibitors. *Bioorg. Med. Chem. Lett.* **2001**, *11*, 1647–1650.
(15) Janetka, J. W.; Ledford, B. E.; Mullican, M. D. Pentacyclic Compounds Useful as Inhibitors of Hepatitis C Virus NS3 Helicase. Patent WO 00/24725, 2000.
(16) Sarno, S.; Reddy, H.; Meggio, F.; Ruzzene, M.; Davies, S. P.; Donella-Deana, A.; Shugar, D.; Pinna, L. A. Selectivity of 4,5,6,7-tetrabromobenzotrizole, an ATP site-directed inhibitor of protein kinase CK2 (casein kinase-2). *FEBS Lett.* **2001**, *496*, 44–48.
(17) Borowski, P.; Deinert, J.; Schalinski, S.; Bretner, M.; Ginalski, K.; Kulikowski, T.; Shugar, D. Halogenated benzimidazoles and benzotrizoles as inhibitors of the NTPase/helicae activities of hepatitis C and related viruses. *Eur. J. Biochem.* **2003**, *270*, 1645–1653.
(18) Maga, G.; Gemma, S.; Fattorusso, C.; Locatelli, G. A.; Butini, S.; Persico, M.; Kukreja, G.; Romano, M. P.; Chiasserini, L.; Savini, L.; et al. Specific targeting of hepatitis C virus NS3 RNA helicase. Discovery of the potent and selective competitive nucleotide-mimicking inhibitor QU663. *Biochemistry* **2005**, *44*, 9637–9644.
(19) Bachur, N. R.; Yu, F.; Johnson, R.; Hickey, R.; Wu, Y.; Malkis, L. Helicase inhibition by anthracycline anticancer agents. *Mol. Pharmacol.* **1992**, *41*, 993–998.
(20) Shoichet, B. K. Virtual screening of chemical libraries. *Nature (London)* **2004**, *432*, 862–865.

(21) Kuntz, I. D. Structure-based strategies for drug design and discovery. *Science* **1992**, *257*, 1078–1082.
(22) Yao, N. H.; Hesson, T.; Cable, M.; Hong, Z.; Kwong, A. D.; Le, H. V.; Weber, P. C. Structure of the hepatitis C virus RNA helicase domain. *Nat. Struct. Biol.* **1997**, *4*, 463–467.
(23) Kim, J. L.; Morgenstern, K. A.; Griffith, J. P.; Dwyer, M. D.; Thomson, J. A.; Murcko, M. A.; Lin, C.; Caron, P. R. Hepatitis C virus NS3 RNA helicase domain with a bound oligonucleotide: the crystal structure provides insights into the mode of unwinding. *Structure* **1998**, *6*, 89–100.
(24) Kim, D. W.; Kim, J.; Gwack, Y.; Han, J. H.; Choe, J. Mutational analysis of the hepatitis C virus RNA helicase. *J. Virol.* **1997**, *71*, 9400–9409.
(25) Lin, C.; Kim, J. L. Structure-based mutagenesis study of hepatitis C virus NS3 helicase. *J. Virol.* **1999**, *73*, 8798–8807.
(26) Oberhauser, T. A new bromination method for phenols and anisoles: $NBS/HBF_4 \cdot Et_2O$ in CH_3CN. *J. Org. Chem.* **1997**, *62*, 4504−4506.
(27) Boguszewska-Chachulska, A. M.; Krawczyk, M.; Stankiewicza, A.; Gozdek, A.; Haenni, A. L.; Strokovskaya, L. Direct fluorometric measurement of hepatitis C virus helicase activity. *FEBS Lett.* **2004**, *567*, 253–258.
(28) Kuang, W. F.; Lin, Y. C.; Jean, F.; Huang, Y. W.; Tai, C. L.; Chen, D. S.; Chen, P. J.; Hwang, L. H. Hepatitis C virus NS3 RNA helicase activity is modulated by the two domains of NS3 and NS4A. *Biochem. Biophys. Res. Commun.* **2004**, *317*, 211–217.
(29) Tai, C. L.; Chi, W. K.; Chen, D. S.; Hwang, L. H. The helicase activity associated with hepatitis C virus nonstructural protein 3 (NS3). *J. Virol.* **1996**, *70*, 8477–8484.
(30) Tai, C. L.; Pan, W. C.; Liaw, S. H.; Yang, U. C.; Hwang, L. H.; Chen, D. S. Structure-based mutational analysis of the hepatitis C virus NS3 helicase. *J. Virol.* **2001**, *75*, 8289–8297.
(31) Tackett, A. J.; Wei, L.; Cameron, C. E.; Raney, K. D. Unwinding of nucleic acids by HCV NS3 helicase is sensitive to the structure of the duplex. *Nucleic Acids Res.* **2001**, *29*, 565–572.
(32) Blight, K. J.; Kolykhalov, A. A.; Rice, C. M. Efficient initiation of HCV RNA replication in cell culture. *Science* **2000**, *290*, 1972–1974.
(33) Otwinowski, Z.; Minor, W. Processing of X-ray diffraction data collected in oscillation mode. *Methods Enzymol.* **1997**, *276*, 307–326.
(34) Brünger, A. T.; Adams, P. D.; Clore, G. M.; DeLano, W. L.; Gros, P.; Grosse-Kunstleve, R. W.; Jiang, J. S.; Kuszewski, J.; Nilges, M.; Pannu, N. S.; et al. Crystallograph & NMR system: a new software suite for macromolecular structure determination. *Acta Crystallogr.* **1998**, *D54*, 905–921.
(35) Esnouf, R. M. Further additions to MolScript version 1.4, inclunding reading and contouring of electron-density maps. *Acta Crystallogr.* **1999**, *D55*, 938–940.
(36) Nicholls, A.; Bharadwaj, R.; Honig, B. GRASP: graphical representation and analysis of surface properties. *Biophys. J.* **1993**, *64*, 166.

JM8011905